論文 / 著書情報
Article / Book Information

Title	Mixing effects in glass-forming Lennard-Jones mixtures
Authors	L. -C. Valdes,F. Affouard,M. Descamps,J. Habasaki
Citation	J. Chem. Phys., 130, ,
Pub. date	2009, 4
URL	http://scitation.aip.org/content/aip/journal/jcp
Copyright	Copyright (c) 2009 American Institute of Physics

Mixing effects in glass-forming Lennard-Jones mixtures

L.-C. Valdes,[1] F. Affouard,[1,a)] M. Descamps,[1] and J. Habasaki[2]
[1]*Laboratoire de Dynamique et Structure des Matériaux Moléculaires, UMR CNRS 8024, Université Lille I, 59655 Villeneuve d'Ascq Cedex, France*
[2]*Tokyo Institute of Technology, 4259 Nagatsuta-cho, Yokohama 226-8502, Japan*

(Received 13 January 2009; accepted 6 March 2009; published online 17 April 2009)

Mixing effects have been investigated from molecular dynamics simulations at constant number of particles, volume, and temperature on the Kob–Andersen glass-forming Lennard-Jones atomic mixture A_xB_{1-x} for $0 \leq x \leq 1$ compositions. Upon cooling, crystallization is observed for $x \leq 0.5$ and $x \geq 0.9$ compositions. The crystalline states can be described by a quite complex coexistence of voids ($x \leq 0.5$), point defects, and one or two crystal structures which were characterized and found identical to those reported by Fernandez and Harrowell [Phys. Rev. E **67**, 011403 (2003)] from energy minimization. Amorphization is also seen at $0.6 \leq x \leq 0.8$ compositions and it is suggested that both crystal structures, CsCl and fcc-hcp, do not compete at these compositions since only one type of crystalline seed is found in the liquid, either fcc/hcp or CsCl. A significant decrease in the diffusion constants for both *A* and *B* particles is also seen above $x_A \simeq 0.5$. The problem of the extraordinary stability of the model against crystallization is discussed. © *2009 American Institute of Physics*. [DOI: 10.1063/1.3106759]

I. INTRODUCTION

A wide variety of materials of specific interactions and degrees of freedom, when cooled in the liquid phase at a rate sufficiently fast, may avoid crystallization and enters in the so-called supercooled state. In this state, the mobility dramatically decreases by several orders of magnitude for a small temperature change. When the structural relaxation time approximately reaches $\tau \approx 100$ s or the viscosity $\eta \approx 10^{13}$ P, the dynamics become so slow that the liquid transforms to an amorphous solid material, i.e., a glass. The corresponding temperature is usually called as the glass transition temperature T_g. Despite a great interest in the past several decades as evidenced by the developments of many models and theories,[1] the glass transition problem remains elusive and a complete and satisfactory physical understanding of the glass formation has not emerged so far.

The Kob–Andersen (KA) model[2] has been successfully used for several years to understand the complex behavior of supercooled liquids and glasses. The success of this model mainly originates from its great capability to avoid crystallization on the time scale of molecular dynamics (MD) simulations and its intrinsic simplicity since it is composed of a binary mixture of simple atoms interacting through pairwise nonadditive 12-6 Lennard-Jones (LJ) potentials. It thus allowed investigations on a broad temperature domain ranging from high temperature in the normal liquid state to low temperature in the deeply supercooled situation and the glassy state.[3–6] The parameters of the KA interaction potentials are directly inspired from the numerical works performed by Weber and Stillinger on amorphous metal-metalloid alloy $Ni_{80}P_{20}$.[7] In this mixture, the presence of small P atoms among large Ni atoms leads to low free volume and high viscosity, which unfavors crystallization unlike monatomic metals. These effects originate from the strong metal-metalloid bond that particularly favors Ni–P neighboring pairs. The 80:20 composition is of particular interest since it corresponds to a deep eutectic in the Ni–P phase diagram, which is classically associated with the great capability of the mixture to be maintained in the amorphous state at low temperatures. In the KA model, *A* and *B* atoms mimic Ni and P atoms, respectively, of the binary alloy, and parameters of the *A*-*B* potential are specifically chosen to make the *A*-*B* attraction the dominant interaction, i.e., the mutual interaction strength does not follow the Berthelot mixing rule. Indeed, as mentioned by Kob and Andersen,[2] mixing alone is not sufficient to prevent crystallization. In the similar binary LJ mixture developed by Ernst *et al.*,[8] the parameter set in which *A*-*B* interaction is not dominant may lead to crystallization at low temperature. At the mostly used 80:20 composition, the canonical KA model has never been found to crystallize from MD simulations except in a very recent study in which a partial phase separation of *A* and *B* atoms was reported after a quite long run of a few billion time steps.[9] The resulting crystalline state is described as a coexisting pure *A* face-centered-cubic (fcc) crystal and an *AB* CsCl-type crystal consistent with the structure predicted by Fernandez and Harrowell[10] from energy minimization and the different crystal structures of binary LJ solids examined in Refs. 11 and 12.

In previous works,[2–6] mixing has been mainly introduced as a mean to suppress crystallization since simple monatomic liquids may easily crystallize. However, mixing effect itself may significantly affect properties of glass-forming liquids and many binary mixtures show unclear anomalous features which pose serious challenges. In recent years, this problem has motivated interesting investigations that provided some theoretical descriptions of the mixing

a)Electronic mail: frederic.affouard@univ-lille1.fr.

effects. In Ref. 13, positive or negative violation of Raoult's law on the composition dependence of viscosity has been well reproduced from simple models of binary LJ mixtures similar to the KA model but possessing different mutual attractive interaction strengths. Positive and negative deviations from the prediction of Raoult's law were described in terms of structure formation and structure breakage, respectively, upon mixing. The link with the topology of their potential energy landscape properties—the homogeneity of the inherent structures—was also addressed.[14] It is also well known that mixing effect may significantly affect the crystallization capability and that mixtures show a richer variety of structures compared to that of pure liquids.[15] Indeed, in contrast to the 80:20 system, at equimolar composition, the KA model was shown to easily crystallize into an *AB* CsCl-type crystal[10] and a large number of crystal structures for this model were reported by Fernandez and Harrowell.[10]

In the present work, from MD simulations, we specifically investigate the composition dependence of the KA model. We particularly focus on the effect of composition changes on the capability of the model whether to show or not to show crystallization. Calculations were made at a constant volume in order to only focus on thermal interactions and invariant potential energy landscape. As we shall see later, the structure obtained upon cooling can be described by a quite complex coexistence of voids, point defects, and one of two crystal structures which were characterized using global and local orientational order parameters.

II. COMPUTATIONAL DETAILS

In this paper, from MD simulations, we have investigated binary LJ mixtures inspired from the KA model, which has been extensively studied as a glass former.[2–6] The system is composed of a mixture of *A* and *B* particles which possess the same mass and no electrostatic charge. The particles interact via nonadditive shifted LJ potentials $V_{\alpha\beta}(r) = 4\epsilon_{\alpha\beta}[(\sigma_{\alpha\beta}/r)^{12} - (\sigma_{\alpha\beta}/r)^{6}]$ with $\alpha,\beta = A,B$. The parameters $\epsilon_{AA}=1.0$, $\epsilon_{BB}=0.5$, $\epsilon_{AB}=1.5$, $\sigma_{AA}=1.0$, $\sigma_{BB}=0.88$, and $\sigma_{AB}=0.8$ were employed. We used the LJ reduced units with σ_{AA}, ε_{AA}, and m_A as the reference length, energy, and mass, respectively.[16] For all simulations, we employed periodic boundary conditions: a cutoff of 3.0 and a time step of 0.002. The total number of particle is $N=N_A+N_B=280$, where N_A and N_B are the numbers of *A* and *B* particles, respectively. The simulation box is a cubic with the box length equal to 6.1563 and the density ρ is thus 1.2. MD simulations were performed at different compositions of *A* particle $x_A = N_A/(N_A+N_B)$ ranging from 0 to 1 in the *NVT* ensemble where the number of particles *N*, volume *V*, and temperature *T* are kept constant. A Berendsen thermostat was used with a coupling time of 5. The MD simulations have been carried out for the following number of *A* particles: $N_A=0$, 8, 17, 28, 56, 84, 112, 140, 168, 196, 224, 252, 263, 272, and 280. The same cooling procedure was used for all compositions and allowed us to investigate a temperature range from $T=4$ to $T=0.05$. As a first step, the mixture of composition x_A is equilibrated at $T=4$ during 80 000 steps. Upon cooling, 130 000 steps were performed at the following temperatures: 3.5, 3, 2.5, 2, 1.8, 1.6, 1.4, 1.2, 1.1, and 1. Then, the system was cooled step by step from $T=0.95$ to 0.05 by an amount of $\Delta T=0.05$. 400 000 MD steps were made at each temperature. This procedure corresponds to a very fast average cooling of about $\simeq 3.5\times 10^{-3}$ similar to those reported in literature for MD simulations.[17,18] Size effects have been checked by performing additional MD calculations on a model made of $N=2048$ particles at different compositions and density $\rho=1.2$. These simulations do not reveal drastic change in the behavior of the system and only a slight shift in the crystallization and the void formation temperatures were found. Crystal structures formed for the $N=2048$ particles are identical to those obtained for the system composed of $N=280$ particles. Size effects thus do not affect the conclusions of the present work.

In order to investigate crystal formation, the rotationally invariant measure of the crystallinity provided by the so-called bond orientational order parameter proposed by Steinhardt *et al.*[19] and Errington *et al.*[20] is employed. Two atoms are considered to be nearest neighbors if their centers are separated by a distance smaller than a cut-off distance roughly corresponding to the minimum located between the first and the second peaks of their pair distribution function. Such a nearest-neighbor pair forms a so-called "bond" whose direction is characterized by a unit vector $\vec{r}$ in an arbitrary reference system. A set of spherical harmonics $Y_{lm}[\theta(\vec{r}),\phi(\vec{r})]$ is associated with each $\vec{r}$, where θ and ϕ are the polar angles of the bond measured with respect to the reference system. A local order parameter can be defined around every single atom *i* by the quantity,

$$\bar{q}_{lm}(i) = \frac{1}{N_b(i)} \sum_{j=1}^{N_b(i)} Y_{lm}(\vec{r}_{ij}), \tag{2.1}$$

where $\vec{r}_{ij}$ is a unit vector in the direction of the bond between atom *i* and its $N_b(i)$ neighbors *j*. A global average quantity $\bar{Q}_{lm}$ is obtained by summing $\bar{q}_{lm}(i)$ over all atoms *i*. Rotationally invariant global parameter Q_l is obtained by summing $\bar{Q}_{lm}$ over the *m* components as $Q_l = \sqrt{[4\pi/(2l+1)]\Sigma_{m=-l}^{m=+l}|\bar{Q}_{lm}|^2}$. Similarly, one can define a local invariant order parameter q_l from $\bar{q}_{lm}(i)$. For symmetry reasons, the first nonzero values occur for $l=4$ in clusters with cubic symmetry and for $l=6$ in clusters with icosahedral symmetry. In the following, Q_6 was chosen since it is the most sensitive of the bond-orientational order and it produces the largest difference between the liquid and the crystalline phases.[20] $Q_6=0.663$, 0.574, 0.484, 0.510, and 0.353 are predicted for icosahedral, fcc, hexagonal-close-packed (hcp), body-centered-cubic, and simple-cubic crystal symmetries, respectively. All the order parameters vanish for an isotropic liquid $Q_l=0$. In order to identify a crystalline seed in the liquid, the method described in Refs. 15 and 21 was used and it is briefly described here. An alignment of q_6 vectors is shown for a crystalline order, while random orientations are observed in a liquid. Therefore, we calculate the correlation between the local order parameter of different neighboring particles *j* of particle *i* as $\Sigma_{m=-l}^{l} q_{6m}(i)\cdot q_{6m}^{*}(j)$, i.e., the cosine angle between two normalized vectors of co-

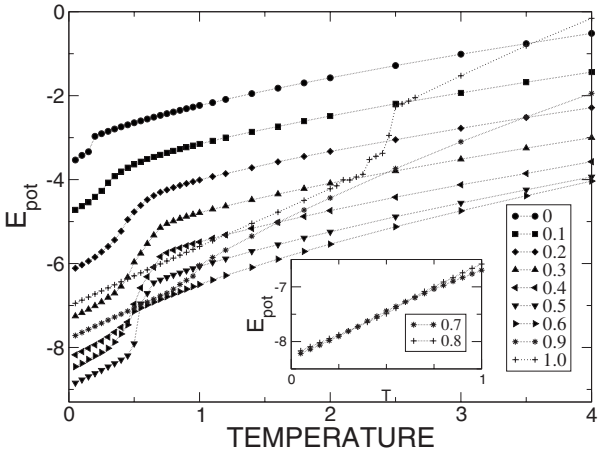

FIG. 1. Potential energy as a function of temperature at different compositions of A particles $x_A=0$, 0.1, 0.2, 0.3, 0.4, 0.5, 0.6, 0.7, 0.8, 0.9, and 1.0 for which energy drop is observed. No energy drop is found at 0.7 and 0.8 (inset).

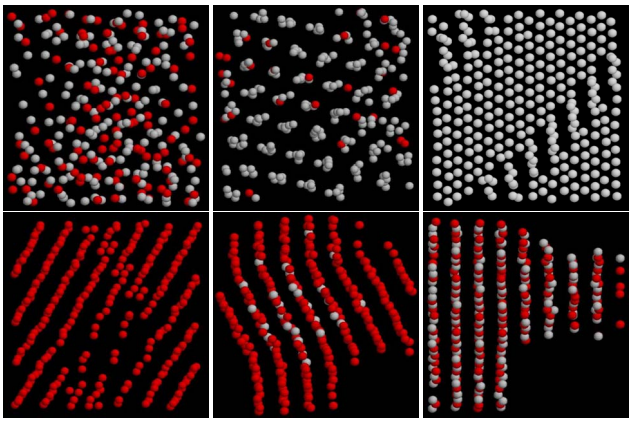

FIG. 2. (Color online) Snapshot of the $x_A=0.0$, 0.1, and 0.5 (bottom, from left to right) and $x_A=0.6$, 0.9, and 1.0 (top, from left to right) mixtures at the temperature of $T=0.05$ obtained after cooling.

ordinates $q_{6m}(i)$ and $q_{6m}(j)$. Particles i and j are considered aligned when this dot product is greater than 0.7. If the number of aligned neighbors of a particle is greater than 5, this particle is taken as a member of a crystalline seed. Particles separated by a distance less than the cut-off distance are considered as belonging to the same crystalline seed.

Liquids under tension may exhibit void formation as cavitation. A precise determination of void space distributions of MD simulated configurations could be made using Voronoi and Delaunay tessellation as shown by Sastry *et al.*[22] for a LJ system. For simplicity, in this work, it is assumed that a void corresponds to the largest spherical region devoid of atoms which can be found in the system. In order to compute the void size radius R_{void}, the MD box is divided into a grid such that the distance between the neighboring grid points is much smaller than the typical first neighbor distance. At every grid point, the distance to the nearest atom is calculated and considered as the void radius at that given grid point. The largest radius value found in the system is taken as R_{void}. It is clear that this method does not allow to investigate shape or the precise distribution of voids. However, from snapshots of several configurations at different compositions and temperatures, it was found that only one void is present in the system of a size fairly estimated by R_{void}. Moreover, void's size is in agreement with the data obtained by Sastry *et al.*[22] on monatomic LJ systems using Voronoi and Delaunay tessellation.

III. RESULTS AND DISCUSSION

Using the cooling procedure described in Sec. II, we have performed quenches of the different mixtures. The potential energy of the different systems as a function of the temperature is shown in Fig. 1. At high temperature or in the vicinity of $T=0$, a smooth and continuous variation in the energy is found as expected for a normal liquid and solid, respectively. At intermediate temperatures, two different scenarios are clearly observed and characterized either by a slow change in slope of the energy for $x_A=0.7$ and 0.8 or by the occurrence of a drop for the other compositions. The slow change in slope is classically associated with the formation of the glassy state and the drop to crystallization. However, in the present case, under the conditions of a fixed density of $\rho=1.2$, the quench procedure may result in configurations in tensioned states (negative pressure) and thus formation of voids.[10,22] Indeed, calculations from energy minimization of the inherent structures of the KA model at $x_A=0.8$ have shown[5] that below a limiting density $\rho\simeq 1.08$, they are spatially heterogeneous and consist of densely packed regions of particles coexisting with voids. Above this density, the inherent structures are spatially homogeneous. As discussed in Ref. 20, energy minimization could be considered as a limit of very fast quenches, so the presence of voids, even it is not expected at $\rho=1.2$ and composition $x_A=0.8$, could be observed at other compositions. From snapshots of the system, below the temperature at which the energy drop is detected, both the existence of crystalline states and the presence of voids are clearly confirmed, as illustrated in Fig. 2.

In the present investigation, we employed the global orientational order parameters proposed by Steinhardt *et al.*[19] Q_6 and its local counterpart q_6 since local disorder is also present. It was thus possible to measure the rate of crystalline phase formed at each temperature and to identify the different crystal structures. These parameters have been calculated for both A and B particles. It should be mentioned that they are usually used to describe orientational order in monatomic liquids but we have also found them relevant to describe binary mixtures in the present study since quite simple crystalline structures are observed. A similar use of these parameters was also reported in Ref. 15 for hard-sphere mixtures. In addition, an estimation of the void size R_{void} was also performed from the simple grid algorithm described in Sec. II. Results are summarized in Table I. Figure 3 shows the evolution of R_{void} and Q_6 as a function of temperature at different selected compositions. For all compositions except $x_A=0.6$, 0.7, and 0.8 for which an amorphous state is found, the final states obtained upon cooling can be described by a quite complex coexistence of voids ($x_A\leq 0.5$), point defects, and one or two crystal structures identical to those reported

TABLE I. Global order parameters Q_6 and radius of the void R_{void} calculated for the structures obtained upon cooling at a temperature of $T=0.05$ for the different x_A compositions (see text). Local order parameters q_4 and q_6 calculated for each particles allow to estimate the values given in parentheses, which indicate the rate of the different crystalline structures. Parameters are always given for the majority species. For the equimolar composition, a similar value is found for A and B particles. Defects are observed in addition to all crystalline phases.

x_A	Q_6	R_{void}	Structure
1.00	0.49	0.9	hcp(0.33)+fcc(0.64)
0.97	0.46	0.8	hcp(0.47)+fcc(0.43)
0.94	0.44	0.8	hcp(0.35)+fcc(0.49)
0.90	0.36	0.8	hcp(0.39)+fcc(0.24)
0.80	0.06	0.9	Amorphous
0.70	0.05	0.9	Amorphous
0.60	0.03	2.0	Amorphous
0.50	0.33	2.0	CsCl
0.40	0.38	1.8	CsCl
0.30	0.30	2.0	fcc+CsCl
0.20	0.36	1.7	fcc+CsCl
0.10	0.43	2.0	hcp(0.10)+fcc(0.49)
0.06	0.40	2.1	hcp(0.35)+fcc(0.27)
0.03	0.40	2.1	hcp(0.44)+fcc(0.28)
0.00	0.45	1.9	hcp(0.38)+fcc(0.47)

by Fernandez and Harrowell[10] from energy minimization. Both onset temperatures of void formation and crystallization are summarized in Fig. 4 as a function of the mixture composition. For the highest compositions $x_A \geq 0.9$, the liquid transforms to a mixture of hcp and fcc phases made of the A species (see Fig. 2). Due to its lowest energy, the hcp structure should be mainly observed compared to the fcc structure. However, in many cases the opposite result is reported in literature (see Ref. 23 and references within). Indeed, as shown in Ref. 23, the energy difference between the hcp and fcc structures is very small and varies with density. It is strongly influenced by slight modifications of the interaction potential such as the value of the truncation cutoff as it is used in the present study. Both hcp and fcc are thus expected to be observed as shown in Ref. 24.

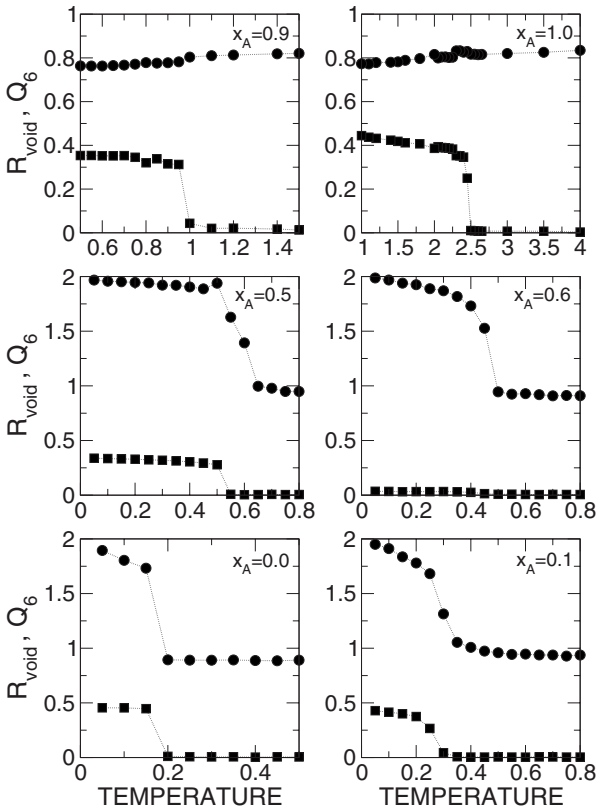

FIG. 3. Void's size R_{void} (circle) and rotationally invariant parameter Q_6 (square) measuring the crystallinity at different compositions $x_A=0$, 0.1, 0.5, 0.6, 0.9, and 1.0.

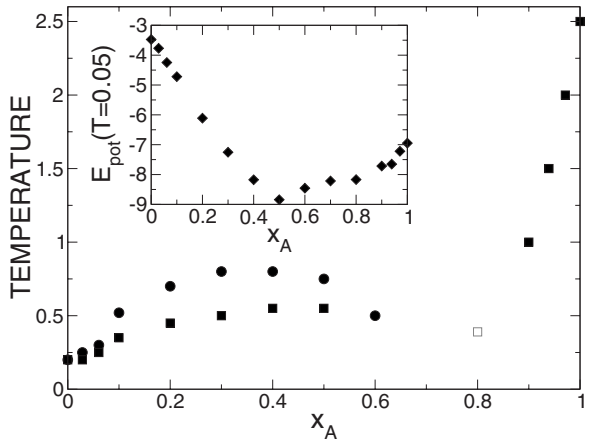

FIG. 4. Phase diagram of the KA model. Onset temperature of void formation (circle) and crystallization (square) are plotted as a function of composition x_A. The crystallization temperature of the standard $x_A=0.80$ KA model is indicated for comparison (Ref. 9). The potential energy at the temperature of $T=0.05$ is given in the inset.

For the pure A system, the final state is mainly composed of hcp and fcc blocks. It possesses the structure found in hard-sphere systems displayed[15] or in homogeneous nucleation of LJ liquids.[24] When only a few B particles are present in the pure A system, they act as simple defects in the global structure and the rate of disorder increases with the composition of the minority species. As shown in Fig. 3 for $x_A=1.0$ and 0.9, R_{void} slightly evolves as a function of temperature around 0.8, showing that no large void is formed. This result is expected since at these compositions the system is under compression ($P=5.2$ at $x_A=0.9$ and $T=0.05$). Voids of small size $R_{void} \simeq 0.8$ naturally exist in liquid and crystalline phases. In fcc and hcp crystalline structures, they just correspond to empty space centered at tetrahedral or octahedral interstices. The main difference between the small and the large voids comes from the fact that it is not possible to insert another LJ atom of size σ in the small voids without overlap with the other atoms in the surrounding. Thus, the condition $R_{void} < \sigma$ or $R_{void} > \sigma$ allowed us to distinguish the expected small voids and the larger voids originating from tension, respectively. For $x_A=0.6$, 0.7, and 0.8, the final states are clearly amorphous with $Q_6 \simeq 0$, as reported in Table I. At the $x_A=0.6$ composition, the system is under tension, $P=-3.7$ at a temperature just above the energy drop. Figure 3 clearly shows the formation of a large void from the liquid and no crystallization since the Q_6 parameter remains extremely small at all temperatures. This behavior is similar

to the formation of spatially heterogeneous inherent structures obtained from energy minimization at the canonical composition of the KA model $x_A=0.8$ and lower density $\rho < 1.08$.[5] This result also means that the limit density should be higher than 1.2 at $x_A=0.6$. At $x_A=0.5$, the liquid easily transforms to the CsCl crystalline phase in agreement with the results mentioned in Refs. 9 and 10. However, it should be noted that an important increase in R_{void} reveals the formation of a large void as observed at $x_A=0.6$ prior to crystallization. These large voids are also formed for all the lower compositions. The system at the $x_A=0.4$ composition exhibits a similar behavior as seen at 0.5 but with a higher disorder. At $x_A=0.3$ and 0.2, quite disordered states are also obtained, which are difficult to characterize precisely using the calculations of the global and local order parameters Q_6 and q_6. As shown in Refs. 25 and 26, this is due to the fact that some structural parameters are highly sensitive to even slight distortion of local structures. It is thus difficult to distinguish between different structures and additional investigations should be necessary. From the present study, the low temperature states at $x_A=0.3$ and 0.2 seem to be composed of a mixture of fcc and CsCl crystalline structures as obtained in Ref. 15 for hard-sphere mixtures. For the lowest compositions $x_A \leq 0.1$, similar features of the $x_A \geq 0.9$ are found. In this situation, a mixture of hcp and fcc crystal phases composed of the B particles (see Fig. 2) is formed in which the remaining A particles play the role of defects. It should be mentioned that for the lowest or highest compositions, the number of A or B minority particles is so low that the formation of CsCl aggregates is highly improbable.

At $x_A \leq 0.5$, both formation of void and crystallization are detected and one may ask if both phenomena are related. A closer look at the evolution of Q_6 and R_{void} as a function of temperature for these compositions indicates that the onset of crystallization occurs once the large void is mainly formed. With the formation of such of void in the structure, a dense local packing of particles appears and is certainly favorable to the crystallization. A proper study of the crystallization mechanisms, determination of the crystal nucleation barriers, and the role of the void formation might be very interesting but it is beyond the scope of the present work, as it requires additional consuming calculations which will be discussed elsewhere.

As previously mentioned, at the compositions $x_A=0.6$, 0.7, and 0.8, no crystallization is observed, while mixtures easily crystallize for the other compositions. In order to understand this unclear difference, we investigated the local structure of the liquid at $x_A=0.6$, 0.7, and 0.8. Using the local orientational parameter q_6 and the method for searching small solid aggregates described in Refs. 15 and 21, it was possible to identify infrequent small crystalline nuclei of about 10 particles which are transiently formed in the liquid and do not grow (see Fig. 5). For $x_A=0.6$, these seeds are found mainly composed of the CsCl structure. It should be noted that a significant increase in the number of particles belonging to these seeds is observed at the temperature corresponding to the void formation. This result confirms that void formation may help crystallization, as suggested above. For $x_A=0.7$, the size of the aggregates remains small and no change is seen as a function of the temperature. These seeds are found to be mainly composed of fcc/hcp and heterogeneous structures. Interestingly, for $x_A=0.8$, the seeds are particularly richer in species A than the equilibrium composition of the liquid and mainly possess fcc/hcp structure (see Fig. 5). The number of particles of the crystalline seeds slightly increases and shows a maximum close to the temperature at which a partial phase separation is reported in Ref. 9 after a few billion steps and for which the resulting state was described as a coexisting pure A fcc crystal and an AB CsCl-type crystal.

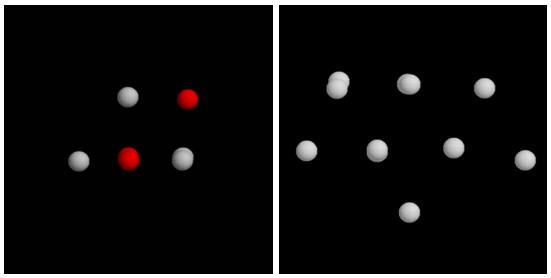

FIG. 5. (Color online) Snapshot of some crystalline aggregates found at $x_A=0.6$ (left) and $x_A=0.8$ (right).

Therefore, we do not observe evidence of competing influence of fcc/hcp and CsCl during nucleation processes since only one type of crystalline seeds is found at the different concentrations: $x_A=0.6$, 0.7, and 0.8. Discussion by free energy should be necessary to fully understand this problem. However, the value of the potential energy obtained at low temperature from the present fast cooling rate is informative (see inset in Fig. 4). Indeed, by comparing the values of the potential energy at the lowest temperature of $T=0.05$, glasses at concentrations of $0.6 \leq x_A \leq 0.8$ are found to be more stable than the crystalline states at $x_A \geq 0.9$ but are less stable compared to the crystalline states for $x_A \leq 0.5$. Randomness such as distribution of coordination number in glasses, which minimizes a local energy, seems to be an inevitable choice of the system for $0.6 \leq x_A \leq 0.8$ because the amount of B seems to be too small to form CsCl-type structure of 1:1 ratio of A and B, while the formation of fcc/hcp makes the system unstable. If large fluctuation of concentration is allowed by annealing or slow cooling rate, the formation of CsCl might begin and allow the formation of other types of crystals as found in the simulation with seed of CsCl-type reported in Ref. 10. Kinetic reason may be also important to explain the noncrystallization since the work by Fernandez and Harrowell[10] showed that the development of crystalline order, mainly fcc arrangements of A particle, remains extremely slow at $x_A=0.8$ composition even with the existence of the CsCl seed. Diffusion coefficients of both A and B particles, noted as D_A and D_B, respectively, which have been calculated at different concentrations x_A are displayed in Fig. 6. They were calculated at different temperatures above crystallization and void formation temperatures. Figure 6 clearly reveals an important decrease in the diffusion when the concentration increases above $x_A \simeq 0.5$. This decrease reaches about two decades at $T=0.8$. Below $x_A \simeq 0.5$, both D_A and D_B do not show significant change. This

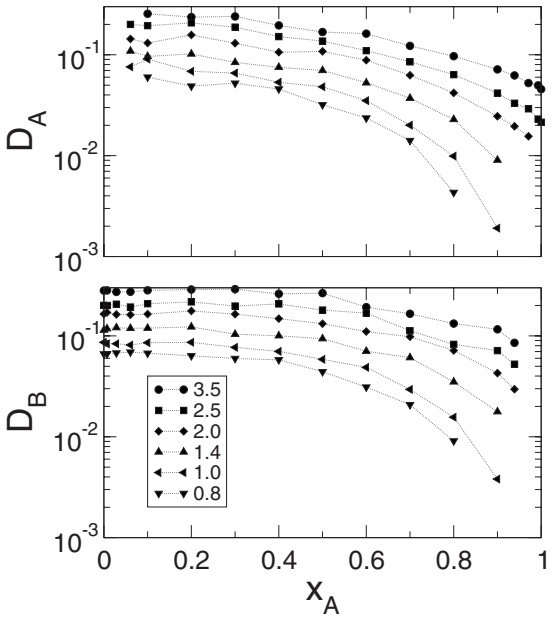

FIG. 6. Diffusion constant of A and B particles as a function of the composition x_A at different selected temperatures $T=3.5$, 2.5, 2.0, 1.4, 1.0, and 0.8 chosen for clarity.

result confirms the difficulty of cooperative arrangements for nucleation and growth in the concentration domain $0.6 \leq x_A \leq 0.8$ and thus may affect the stability of the glass to crystallization.

IV. SUMMARY AND CONCLUSIONS

In summary, KA mixtures at different compositions and temperatures have been investigated from MD computer simulations in the *NVT* statistical ensemble. Upon cooling, crystallization is observed for $x_A \leq 0.5$ and $x_A \geq 0.9$ compositions. However, a unified crystal does not arise. Instead, there results a complex polycrystalline structure with the presence of large voids since some of the low temperature states are under tension. The crystal formation and the crystal structures were characterized using a rotationally invariant measure of the crystallinity provided by the bond orientational order parameters. Fcc-hcp mixtures were found at the highest and the lowest compositions, while pure CsCl and CsCl-fcc mixtures were obtained close to the equimolar compositions. Amorphization is seen at compositions $x_A = 0.6$, 0.7, and 0.8. It is suggested that both crystal structures, CsCl and fcc-hcp, do not compete for nucleation since only one type of crystalline nuclei possessing either fcc/hcp at $x_A=0.7$ and 0.8 or CsCl $x_A=0.6$ is found. Crystallization seems inhibited because (i) the fcc/hcp structure is less stable than the glass which is itself less stable than the CsCl structure and (ii) the number of B particles is too small to form the CsCl structure. Moreover, a drastic decrease in the diffusion constants for both A and B particles is also found above $x_A \simeq 0.5$ which certainly unfavors large fluctuations of concentration and contributes to the extraordinary stability of the model to crystallization.

As a rational step, before one proceeds with other studies, it was essential to calculate the solid-liquid phase diagram and the structure of the crystal states of the system. This work was performed in the present investigation. For future studies, we would like to investigate the mechanisms of crystal nucleation in these mixtures using the methods described in Ref. 21 and also the influence of the quenching rate. It would be interesting to determine if crystal nucleation is preceded by fractionation of the components which increases the free energy barriers for phase transition as demonstrated for hard-sphere mixtures in Ref. 15.

ACKNOWLEDGMENTS

The authors wish to acknowledge the use of the facilities of the IDRIS (Orsay, France) and the CRI (Villeneuve d'Ascq, France) where calculations were carried out. This research was partly supported by the Ministry of Education, Science, Sports and Culture, Japan, Grant-in-Aid for Scientific Research (C) (Grant No. 19540396), 2007-2009.

[1] P. G. Debenedetti and F. H. Stillinger, Nature (London) **410**, 259 (2001).
[2] W. Kob and H. C. Andersen, Phys. Rev. E **51**, 4626 (1995).
[3] W. Kob, C. Donati, S. J. Plimpton, P. H. Poole, and S. C. Glotzer, Phys. Rev. Lett. **79**, 2827 (1997).
[4] F. Sciortino, W. Kob, and P. Tartaglia, Phys. Rev. Lett. **83**, 3214 (1999).
[5] S. Sastry, Phys. Rev. Lett. **85**, 590 (2000).
[6] P. Bordat, F. Affouard, M. Descamps, and F. Müller-Plathe, J. Phys.: Condens. Matter **15**, 5397 (2003).
[7] T. A. Weber and F. H. Stillinger, Phys. Rev. B **31**, 1954 (1985).
[8] R. M. Ernst, S. R. Nagel, and G. S. Grest, Phys. Rev. B **43**, 8070 (1991).
[9] S. Toxvaerd, T. B. Schroeder, and J. C. Dyre, e-print arXiv:cond-mat/0712.0377.
[10] J. R. Fernandez and P. Harrowell, Phys. Rev. E **67**, 011403 (2003).
[11] M. Vlot, H. Huitema, A. Vooys, and E. van der Eerden, J. Chem. Phys. **107**, 4345 (1997).
[12] T. F. Middleton, J. Hernandez Rojas, P. N. Mortenson, and D. J. Wales, Phys. Rev. B **64**, 184201 (2001).
[13] A. Mukherjee, G. Srinivas, and B. Bagchi, Phys. Rev. Lett. **86**, 5926 (2001).
[14] S. E. Abraham, D. Chakrabarti, and B. Bagchi, J. Chem. Phys. **126**, 074501 (2007).
[15] S. Punnathanam and P. A. Monson, J. Chem. Phys. **125**, 024508 (2006).
[16] *Computer Simulation of Liquids*, edited by M. P. Allen and D. J. Tildesley (Oxford Science, Oxford, 1987).
[17] T. Keyes, Phys. Rev. E **59**, 3207 (1999).
[18] J. Buchholz, W. Paul, F. Varnik, and K. Binder, J. Chem. Phys. **117**, 7364 (2002).
[19] P. J. Steinhardt, D. R. Nelson, and M. Ronchetti, Phys. Rev. B **28**, 784 (1983).
[20] J. R. Errington, P. G. Debenedetti, and S. Torquato, J. Chem. Phys. **118**, 2256 (2003).
[21] S. Auer and D. Frenkel, J. Chem. Phys. **120**, 3015 (2004).
[22] S. Sastry, P. G. Debenedetti, and F. H. Stillinger, Phys. Rev. E **56**, 5533 (1997).
[23] A. N. Jackson, A. D. Bruce, and G. J. Ackland, Phys. Rev. E **65**, 036710 (2002).
[24] H. Wang, H. Gould, and W. Klein, Phys. Rev. E **76**, 031604 (2007).
[25] J. P. Neirotti, F. Calvo, D. L. Freeman, and J. D. Doll, J. Chem. Phys. **112**, 10340 (2000).
[26] W. Polak and A. Patrykiejew, Phys. Rev. B **67**, 115402 (2003).